sustainability

MDPI

Article

An Incremental and Philosophically Different Approach to Measuring Raster Patch Porosity

Tarmo K. Remmel

Department of Geography, York University, 4700 Keele Street, Toronto, ON M3J 1P3, Canada; remmelt@yorku.ca; Tel.: +1-416-736-2100

Received: 23 July 2018; Accepted: 22 September 2018; Published: 25 September 2018

check for updates

Abstract: A new method for measuring the porosity of individual 2D raster patches in a GIS for characterizing the combined complexity of a shape's edge in conjunction with its internal perforations is developed. The method is centered on comparing the number of cellular edge–edge joins relative to the theoretical maximum number of similar joins possible given a set number of cells comprising a landscape patch. As this porosity (Φ) increases, the patch (or shape) can be viewed as deviating from a maximally compact form, comprising higher edge complexity and internal heterogeneity (inclusion of perforations). The approach is useful for characterizing shapes for which a simple perimeter- or area-based metric misses the internal complexity and where the porosity of the patch may provide insight into spatial processes leading to the development of the landscape fabric. I present theoretical results to illustrate the mechanics of the approach and a small case study of boreal wildfire residual vegetation patches in Ontario, where real resulting wildfire process-driven landscape patches are assessed for their porosity at five spatial resolutions. The results indicate that naturally occurring and unsuppressed boreal wildfires in the study area typically produce residual vegetation patches with an average porosity of 17.6%, although this value varies slightly with the spatial resolution of the data representation.

Keywords: planar; binary pattern; patch; perforation; shape; complexity

1. Introduction

Mapping land cover and its changes is central to landscape analyses and for establishing baseline conditions, formulating hypotheses of landscape change, and understanding processes of transition, disturbance, or landscape alteration. Tracking such fundamental landscape elements is also important for identifying the successes and failures of conservation efforts and in developing sustainability goals and guidelines, as they provide a spatial mapping of landscape state [1–3]. The subsequent computation of landscape-, class-, or patch-level metrics seeks to further quantify landscapes and to produce robust and repeatable measurements of landscape states and patterns [4]. While numerous metrics exist across the three levels of measurement, the number of patch-level metrics pales in comparison to the others, and specifically lacks a metric focused on the structural level of individual patch-forming cells. Such an emphasis on individual patches allows landscape entities that are relatively rare but highly localized and form their own environment (e.g., wildfire) to be assessed as a unit rather than as an extreme among an otherwise continuous uniform landscape matrix.

Porosity has long been used to describe a characteristic of many materials. In simple terms, porosity characterizes the volume of voids relative to the volume of the mass that contains them. Porosity characterizes the amount of a material's mass relative to its volume, often given as a percentage or as a proportion. A material having high porosity will have a greater proportion of its volume comprised of voids than a material with low porosity. This measure often correlates with density and other physical characteristics and processes, such as buoyancy, permeability, or heat transfer [5,6].

While often considered as a metric computed for a three-dimensional volume of some material, the concept can be generalized to two-dimensional planar shapes containing perforations [7,8]. Imagine a slice of Swiss cheese—porosity can be computed to provide the proportional area of the holes that were formed by gas bubbles with respect to the total area of the slice. By extension, the gaps within an otherwise-intact forest canopy, as drawn on a flat map, can be described by a two-dimensional notion of porosity as if it were a porous membrane or plane [9,10]. This paper focuses solely on the concept of two-dimensional porosity, specifically considering the representation of spatial phenomena stored in a geographic information system (GIS).

The storage of spatial entities (e.g., forest stands, bodies of water) in a GIS requires many decisions regarding how they will be represented, and each decision will influence any secondary measurements made of those entities [11,12]. Most often, arguably the coarsest level of representation that must be decided is whether a vector or raster data model will be used [13]. Since raster data from satellite images [14], digital or scanned aerial photographs [15], spatial models [16], and simulations [17] form the foundations of countless spatial analyses, and because we continually seek to measure and summarize the complexity of shapes and patterns observed in this context [18–21], the raster model is a logical starting point for such a discussion. Further, the raster data representation model is simpler than the vector model in that the partitioning of geographic space in raster is controlled (equally sized and spaced cells) as compared to the variable spacing of points (nodes and vertices) in a vector model. Thus, from a spatial uncertainty and variability perspective, the constrained scope and complexity of the raster model offers the simpler case between the two representational models. Finally, given the prevalence of raster data for ecological studies [22], scaling studies [23], and forest research [24] (areas with which I have substantive familiarity), I will focus only on the raster data model in this current work, understanding that extensions to vector can logically follow afterward.

Redundancies among landscape metrics (i.e., highly correlated metrics that differ primarily due to a scaling factor) are known, and while mitigative approaches have been proposed (e.g., [25,26]), there remain challenges with interpreting and comparing numerous landscape metrics [27–29]. Since landscape metrics typically have non-normal distributions that are further influenced by the complex interactions between composition and configuration, quantifications are often abstract and not indicative of any unique state but an exceptionally broad range of possible compositions and configurations, and are likely more useful as generic indicators or diagnostic tools [27,30]. As such, alternate and palpable options for comparing categorical maps have been developed (e.g., [31–33]) and metrics that segment landscapes into tangible morphological elements (each cell belonging to a single morphological class), along with their summaries, are becoming increasingly attractive [34,35] and are easily visualized and mapped.

Motivated by such tangibility, the identification, measurement, and quantification of shapes and characteristics of individual landscape elements (hereafter referred to as "patches", to follow terminology borrowed from landscape ecology) that can be subsequently summarized across a wider extent if required, rather than the production of single metric values for landscapes or classes that dilute the infinite complexity of an entire landscape [36] are gaining attention. In this way, morphological analyses [35] produce segmentations of binary landscapes (e.g., forest versus non-forest), placing individual cells into discrete and mutually exclusive structural element classes (e.g., core, edge, perforation) that have concrete meaning and which can be easily mapped [37]. I argue that these morphological elements not only describe the structure of a landscape but provide elements that are easily visualized and understood, even by non-specialists. Given the frequency distributions of these morphological elements, mapped realizations of these distributions can be drawn. These properties make them highly favourable for communication among specialists and generalists alike.

When individual landscape patches become the scope of landscape pattern analyses and characterizations, tools for assessing patch-level metrics [19] and also more detailed multi-variate summaries of shape [38,39] become increasingly suitable over class- or landscape-level metrics. Furthermore, the contributions by individual morphological elements to complex landscape objects or entities allow fine-scale and multi-scale characterization and interpretation [40]. Some landscape features may contain hierarchically nested and related morphological elements (e.g., small lakes on an island within a larger lake situated in a forested landscape) that may be considered as perforations (i.e., holes or voids) that will vary depending on the context and scope. It is possible to assess the structures, shapes, and characteristics of these patches individually or collectively. Thus, a landscape patch may express emergent properties that can be described at multiple scales and across varying contexts [41] or with fractal properties [42] (i.e., having elements of self-similarity when measured across spatial scales).

In this paper, I develop a metric for quantifying the porosity of a planar feature, an individual patch, represented in a raster GIS as the porosity summarizes the total complexity of a shape (edge and internal characteristics together), rather than just its outer perimeter or interface with the landscape matrix or other landscape patches. Specifically, I build the logical thinking behind the metric, and provide examples of its use in characterizing boreal post-fire residual forest stand structures. I demonstrate the impact of spatial resolution on this metric and indicate how the porosity can provide information that augments typical area, perimeter, area-to-perimeter ratio, and shape summaries. The proposed metric is also highly tangible, meaning that it can be easily visualized due to its non-abstract nature.

As in Figure 1, assume that a foreground spatial feature (i.e., a residual forest stand) is mapped as 1s relative to the background matrix (i.e., wildfire burned area) which is mapped as 2s onto a regular grid of cells with a fixed spatial resolution (R). In this case, each cell has an area (A) equal to R^2. An isolated cell (i.e., a single cell (1) surrounded completely by background (2)) would have a perimeter (P) equal to $4R$ (Figure 1a). As an increasing number of residual forest stand cells are mapped contiguously, then $A = n{\cdot}R^2$, where n is the number of contiguous cells (Figure 1b). Contiguity is determined a priori by selecting either a 4- or 8-neighbour rule [43] that determines whether neighbours exist when they share an edge (Rook's case), or whether cells that touch corner-points are also considered as contiguous (Queen's case) (Figure 1c). A cell's membership in a landscape patch is thus completely determined by contiguity and not by defining an enclosing area by methods like a minimum convex polygon or an α-hull [44] that have been argued to potentially express substantial area bias, particularly for deeply incised areas or complex shapes. With the Queen's case, the addition of individual cells to a patch produces a consistent area increase. However, perimeter length does not scale as nicely, since the degree of porosity and the number and types of contacts with other cells will influence the length of the perimeter. In this study, the 8-neighbour contiguity is implemented to capture all like-cover-dominated cells that touch in any way into individual patches.

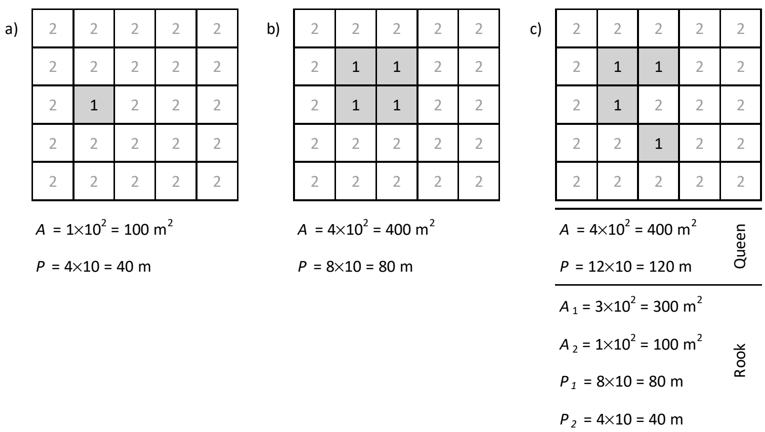

Figure 1. Residual forest (1) and burned matrix (2) mapped onto a regular grid with a spatial resolution of 10 m. An isolated cell (**a**); four contiguous cells forming a highly compact feature with either the Rook's or Queen's neighbour rule (**b**); and either one residual forest patch with the Queen's case, or two non-contiguous residual forest patches with the Rook's case (**c**).

Traditionally, the compactness of an individual patch has been assessed by the perimeter-to-area ratio (P/A) which is also a proxy of shape complexity [45]. The idea behind this ratio is that maximally compact shapes will have the shortest perimeter possible to contain the area (e.g., a circle or square in vector or raster representations, respectively). High positive spatial autocorrelation reinforces the fact that like things cluster and thus increase compaction [46–48]. While conceptually simple, this approach neglects to compensate for scale (i.e., the area of a patch will influence the resulting P/A ratio), where a larger patch will have a relatively smaller ratio than a smaller patch would, both being equally compact (see [38] for a more detailed review). This leads to the use of any number of corrected perimeter-to-area ratios (cP/A) (see [49] for some options), where correction factors compensate for scaling). In one classic example (Equation (1)), a perfect circle would have cP/A = 1.000 (suitable for use with vector data), and a square would have cP/A = 1.128 (for use with raster data), regardless of the patch's area. Software tools such as Fragstats [19] offer several patch-level metrics such as CONTIG (contiguity index), PARA (perimeter-area ratio), FRAC (fractal dimension index), CIRCLE (related circumscribing circle), and SHAPE (shape index) that measure aspects of shape and patch complexity, but I demonstrate that the proposed porosity metric presented in this paper offers an alternative and structurally different option based on accounting for a contact perimeter ratio. The concept of comparing a patch shape to its maximally compact form given the number of cells that comprise it provides a good reference point for a new metric, as it will be stable relative to its area.

$$cP/A = \frac{0.282 \cdot P}{\sqrt{A}} \tag{1}$$

If we expand our scope beyond a single entity to a larger landscape, then class- and landscape-scale metrics begin to emerge as useful tools to capture processes acting across multiple patches as in percolation theory [50]. Percolation theory in a raster GIS context can be visualized as a layer comprising a single class (e.g., forest = 1), where individual cells subsequently and randomly get converted to another class (e.g., non-forest = 0). At some point, that new, non-forest class will connect across the entire original scene, thereby fragmenting the original contiguous forest area. This has been shown to occur when the critical compositional proportion reaches 0.5829 [51] (more recently this value has been better assessed to be 0.592 by [52]) and connects multiple landscape patches into one super-patch. Critical values such as this have been studied in ecology that infer the effects of forest fragmentation on things such as bird and animal habitats, but at much lower thresholds due to the non-random nature of the processes involved [53]. I translate this concept to an individual patch, whereby properties of that patch will change as it becomes increasingly perforated or experiences an increased edge complexity.

Fahrig [54] discusses fragmentation effects on biodiversity and distinguishes between habitat loss and fragmentation, where the latter is the specific case of the breaking apart of habitat. Whether percolation, fragmentation, or loss processes are involved, they each indicate that landscape entities are not necessarily compact, isolated, and stable through time. Any landscape or patch comprising that landscape can become perforated and have its edges reshaped by eroding or dilating them. As such, a measure that quantifies the edge and internal complexity of a landscape patch as deviation from maximum compactness (i.e., the proposed measure of porosity) is warranted, since perimeter, area, and shape are not the only characteristics that may be of interest to a practitioner. The comparison with maximum compactness allows for controlling for a shape's size and scale, providing a reference number of joins related directly to the compositional structure of the patch at a given scale.

In this paper, I present some theoretical results for constructed landscape entities to demonstrate the utility of the presented metric. I then compute porosities for residual boreal forest vegetation patches that escaped burning in naturally occurring wildfires from Northern (boreal) Ontario and compare the results with some of the leading patch-level metrics available [55].

2. Materials and Methods

When considering a landscape patch mapped as a series of n cells on a regular grid, Bribiesca [56] describes contact perimeters as the cell edges that touch within the defined patch (Figure 2). Assessing connectivity by identifying contact perimeters (joins) is strongly rooted in join-count statistics, and has been used to assess whether or not frequencies of join types on binary raster maps are within expected limits for the assessment of spatial randomness versus clumpiness [57]. This extends to the computation of the maximum measure of discrete compactness, $J_{\max}$ (Equation 2), that provides the number of contact perimeters expected for a maximally compact shape formed by n cells [49,56,58]. Here "truncate" means to drop all values following the decimal place, such that $J_{\max}$ will only represent complete and whole joins. In this paper, I refer to this measure as $J_{\max}$, the maximum possible number of joins among a given number of cells. By definition, this method of counting contact perimeters assumes a Rook's case contiguity (i.e., connectivity is based on a 4-neighbour rule). However, any method could be used to initially extract cells that could be considered as belonging to a single landscape patch that is subsequently processed in this way.

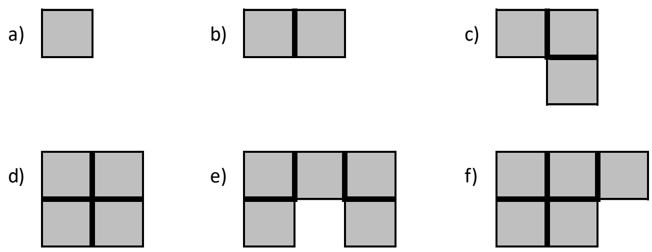

Figure 2. Six raster entities comprised of a varying number of cells. The number of contact perimeters (bold) are 0, 1, 2, 4, 4, and 5 respectively when going from (**a**–**f**). The $J_{\max}$ values for these cases are 0, 1, 2, 4, 5, and 5 respectively.

$$J_{max} = truncate\left[\frac{4n - 4\sqrt{n}}{2}\right] \tag{2}$$

Since $J_{\max}$ provides the maximum number of possible joins among n cells, it becomes possible to measure the actual number of contact perimeters or joins within a landscape patch (J_{act}) with n cells and then to compare that against the maximum expected for the same number of n cells. Deviation from $J_{\max}$ indicates a lack of perfect compactness due to the existence of perforations or increased edge complexity (which can be conceptualized as edge erosion) that together contribute to increased porosity. Thus, the ratio of the actual number of joins to the theoretical maximum for a patch with a set n cells is a measure of that shape's porosity, Φ (Equation 3). If J_{act} and $J_{\max}$ are the same value, then the ratio between them is 1, and therefore $1 - 1 = 0.0$, or no porosity—the shape is maximally compact. However, as J_{act} decreases relative to $J_{\max}$, the ratio decreases, and the porosity value begins to increase, indicating the degree of deviation from maximal compactness. This ratio can be multiplied by 100 to obtain it as a percentage if desired.

$$\Phi = 1 - \frac{J_{\text{act}}}{J_{\max}} \tag{3}$$

For the Ontario boreal wildfire dataset of 11 fire events (see details in [59]), I computed porosity using *arcpy* for ArcMap and the leading patch-level metrics available in Fragstats (i.e., CONTIG, PARA, FRAC, CIRCLE, and SHAPE) [55]. The results were combined and then further processed in R [60] to demonstrate similarities, differences, and the impact of spatial resolution among the metrics. All patches were defined using 8-neighbour (Queen's case) contiguity followed by the subsequent computation of metrics. All computations were performed separately at 4, 8, 16, 32, and 64 m spatial resolutions as produced by [59] to represent a cross section of typical commercial remote sensing data options.

I present both theoretical and actual results to demonstrate the use of this new porosity metric on 2D raster landscape entities. The theoretical shapes were constructed to show a range of possible cell configurations forming patches with the Queen's contiguity rule, and some incorporate voids and porosity because they were not maximally compact. The second set of results was based on the set of mapped boreal wildfire residuals from [59]. Details related to the imagery, processing, and classification are all detailed in that paper, but to summarize, I used binary maps of undisturbed cells within large boreal wildfire events as the base data in this study. Cells deemed contiguous by the Queen's contiguity rule were coded as belonging to a common patch. The patches were drawn from fire footprints of 11 fire events (i.e., F01, F02, . . . F11). These entities were mapped at five spatial resolutions to produce over 6500 representations of unique residual patches (event × resolution combinations). These residual patches have been the focus of sustainable forest management through the action of emulating natural disturbances [61], and a measure of porosity can provide valuable information on how to spatially emulate residual landscape patches in an operational setting. Further details of these residual patches can be obtained from [62,63].

3. Results and Discussion

The first result is for three fabricated landscape patches (Figure 3) mapped with foreground cells in grey, background cells in white, and all edge–edge joins bolded relative to the normal black cell outlines. Note that each of the entities comprised eight foreground cells, but that given differences in their compactness (i.e., their configurations differ), the porosity reflects the degree of deviation from a maximally compact shape. Here, the relatively compact shape in Figure 3a has a single perforation but is otherwise compact and has $\Phi = 0.20$. As an increasing number of cells deviate from ideal compactness (e.g., Figure 3b) the porosity increase, as can be seen from a further erosion of the compact and simple outer perimeter. When all cells are maximally compact, then J_{max} and J_{act} are equal and $\Phi = 0.00$ (Figure 3c). Note that for any given Φ value, dependent on n, there may be ≥ 0 possible cell configurations.

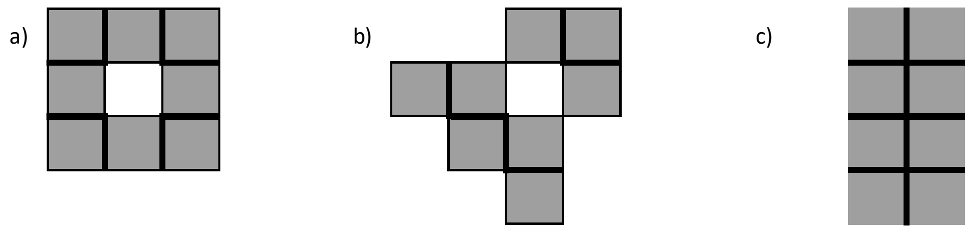

Figure 3. Three landscape entities with contact perimeters (joins) bolded, each has $n = 8$ cells. The porosities for (**a**) through (**c**) are 0.20, 0.40, and 0.00, respectively. Note that (**b**) depicts a shape based on an 8-neighbour contiguity and hence the perforation further increases the measured porosity.

As the number of cells comprising a landscape patch increase, so will the number of possible configurations for a given level of porosity (Figure 4). This is not a limitation of the method, but an indication of what the metric aims to characterize. It is well-known that coarser spatial scales mask local detail and therefore produce simpler shapes with fewer voids [64,65]. For Φ, it matters more what the overall configuration of internal joins looks like (to measure complexity and hence porosity) than the actual shape of the patch. This porosity metric emphasizes the internal and edge complexity with the presence and configuration of perforations to describe the deviance from a maximally compact shape, regardless of its size (based not on area but the number of cells). This reliance on n rather than area means that spatial resolution and the physical unit of measurement is not as important as consistently counting cell joins across any number of cell resolutions. The examples in Figure 4 demonstrate the possible configurations and porosity values possible, for relatively small n. The number of configurations would be further constrained if a 4-neighbour contiguity rule was observed rather than the depicted 8-neighbour contiguity rule. Note that these configurations can be rotated, flipped, or mirrored without altering the porosity values.

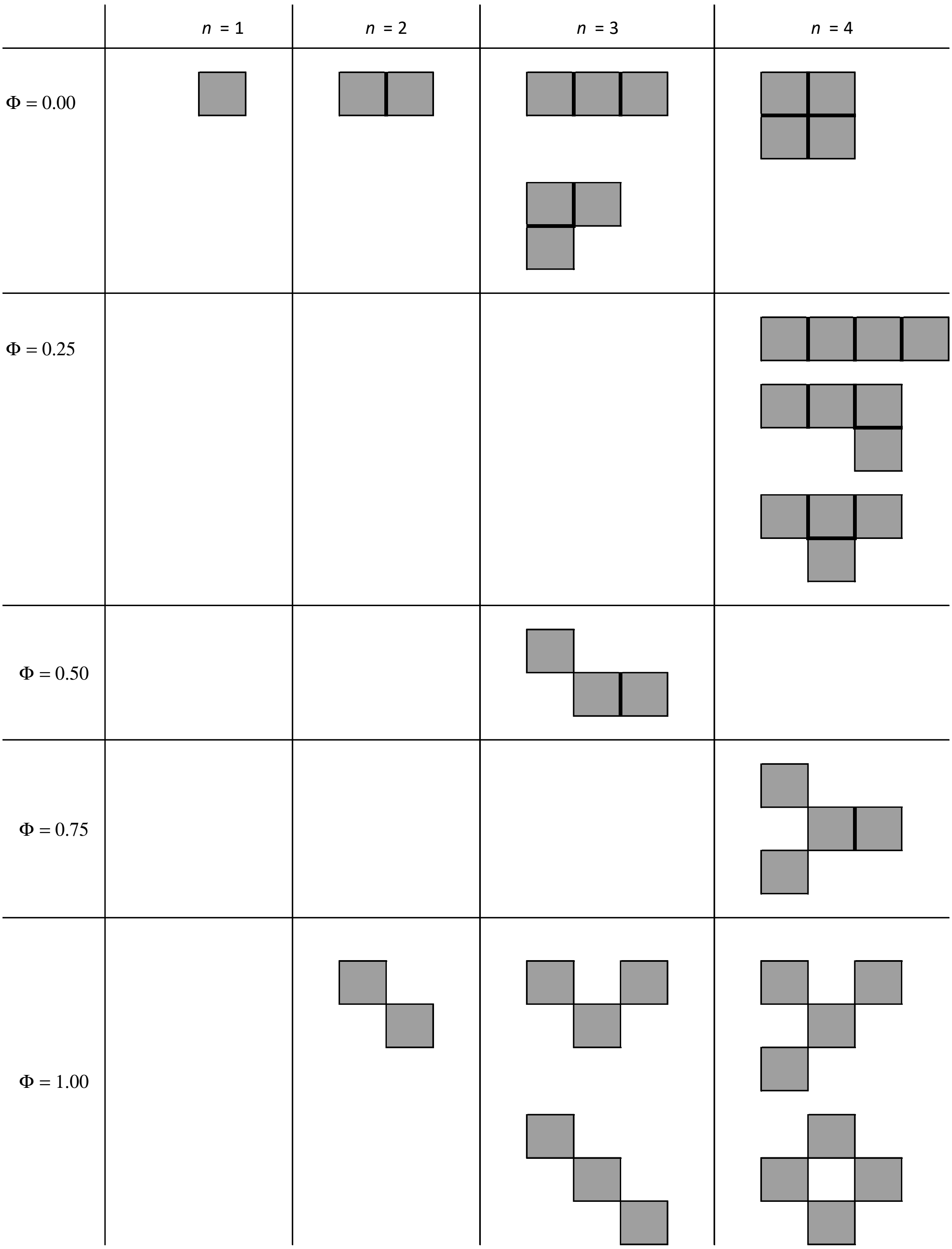

Figure 4. Depiction of all possible landscape patch configurations and their corresponding porosity values for n = 1, 2, 3, and 4 cells under an 8-neighbour contiguity definition.

For the Northern Ontario residual forest patch data, the porosity of each was computed and the results are summarized in Figure 5. These results indicate that while porosity did vary among individual stands, there was relative stability among the 4, 8, and 16 m spatial resolutions. Coarser cells resulted in much greater variability but also generally less porous and thus simpler patch structures.

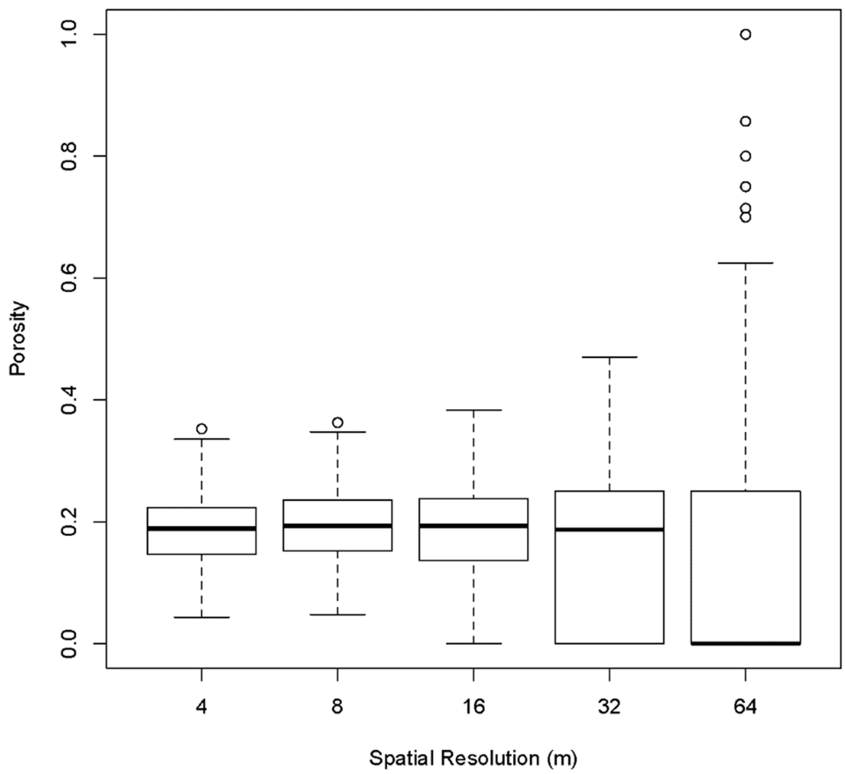

Figure 5. Summary of Ontario boreal wildfire residual vegetation stand porosity mapped at five spatial resolutions.

Porosities were examined among all wildfire events (lumping all spatial resolution classes) to produce Figure 6. While this glosses over the variability introduced by the cell size, the effect of changing spatial resolution was further investigated among wildfire events while separating the individual spatial resolutions. While the graphs are not shown here, a similar trend as in Figure 5 was observed, where coarser spatial resolutions tended towards being non-porous. The most uniform results across wildfire events was found at 16 m spatial resolution—a spatial scale that is about four times as coarse as the Ikonos data from which the analysis stemmed, and finer than the typical Landsat TM/ETM+ analyses that are quite normal for wide-area analyses. Average porosity values at each of the five spatial resolutions within each individual wildfire event are provided in Table 1, the overall average being 17.6% porous. While this figure appears stable in this small example, before it can be made into a recommendation for wildfire disturbance emulation by forest harvesting, a much more geographically extensive ecological study would need to be conducted. Higher spatial resolution representations have a larger number of cells, and thus possible configurations and the ability to capture small perforations. This is reinforced by the 4, 8, and 16 m spatial resolution cases having the highest average perforations. Overall, however, residual patches were generally compact and regardless of the spatial resolution at which they were mapped, most residual patches were formed with reasonable consistency.

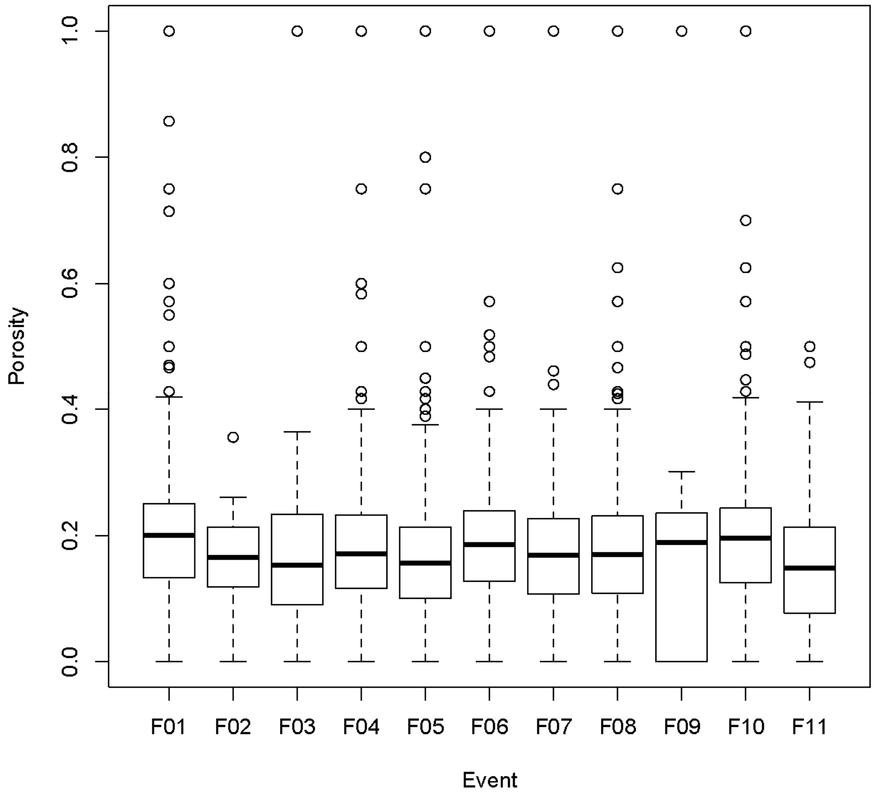

Figure 6. The variability of residual vegetation patch porosity among wildfire events (lumping all five spatial resolutions).

Table 1. Average porosity of wildfire residual vegetation patches within individual fire events, computed for five different spatial resolutions (in metres).

Event	Resolution				
	4	8	16	32	64
F01	0.2129	0.2050	0.2015	0.1593	0.1592
F02	0.1911	0.1769	0.1840	0.1694	0.0200
F03	0.1315	0.1419	0.2144	0.1250	0.3333
F04	0.1693	0.1848	0.1882	0.1569	0.1681
F05	0.1445	0.1776	0.1725	0.1494	0.1500
F06	0.1812	0.2039	0.1991	0.1525	0.1515
F07	0.1529	0.1850	0.1796	0.1657	0.1284
F08	0.1529	0.1867	0.1859	0.1695	0.1659
F09	0.2591	0.1706	0.1826	0.0556	0.3333
F10	0.2084	0.1950	0.1896	0.1688	0.1278
F11	0.1480	0.1699	0.1596	0.1481	0.1137

The histogram summarizing the frequency distribution of porosity values across all spatial resolution classes and fire events (Figure 7) is bimodal. However, two clear cases emerged when the bin of $\Phi = 0.0$ was separated from the rest of the data. The high frequency of $\Phi = 0.0$ represents the large number of small islet-type residual patches. Islets are defined appropriately by Vogt et al. [34] as patches or landscape entities that are not wide enough to contain any core area from a mathematical morphological perspective. These islets can range from $n \geq 1$ cells, but most are quite small and thus compact by their definition. The remainder of the distribution is nearly normal and represents the vast majority of residual patches. Omitting the $\Phi = 0.0$ cases, the average porosity for all wildfire events across the five spatial resolutions rose to 20.9%.

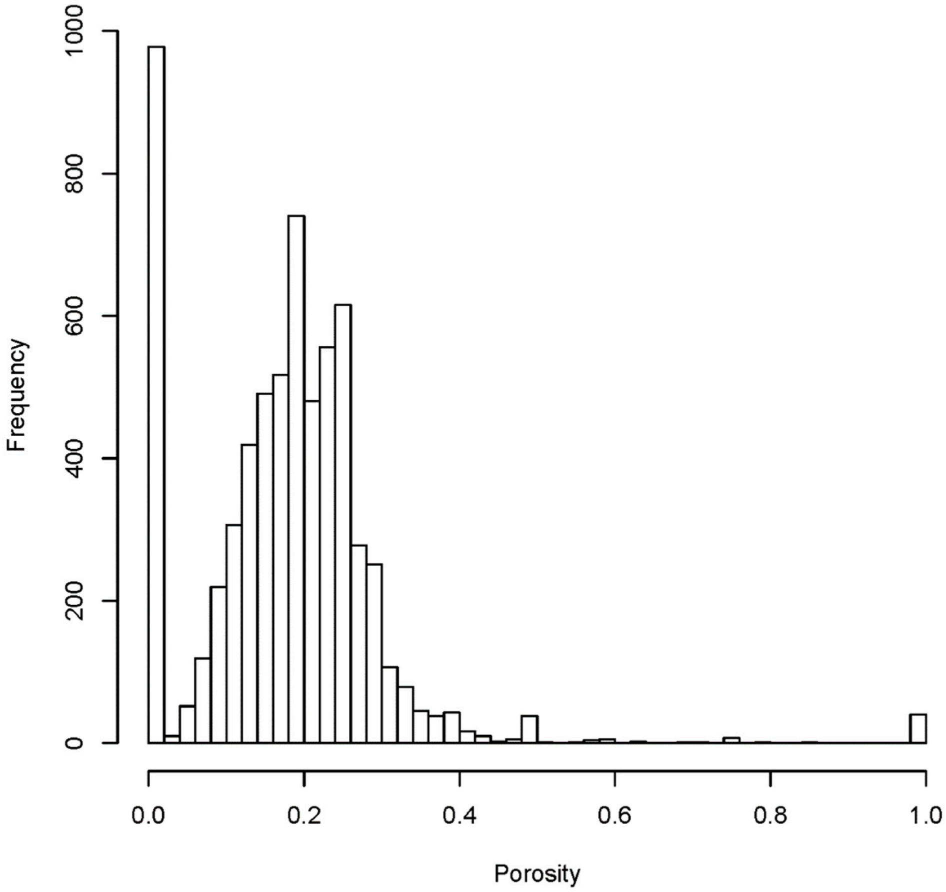

Figure 7. Histogram of porosity values for nearly 6500 residual patches measured.

Scatterplots showing the relationships among these metrics and porosity are given in Figure 8. There were no simple correlations among any of the comparisons, as can be seen by the broad point clouds. While both PARA and FRAC exhibited a degree of influence by spatial resolution, the broad variance in even these subsets indicated that there was substantial variability with the existing metrics. While the strongest relationship was with PARA, I argue that porosity is a fine-tuning of this type of metric which goes beyond simply comparing the area and perimeter of a patch. Porosity summarizes total patch complexity by assessing the number of like joins relative to a normalized maximum for that patch, given the number of cells comprising it. Thus, the porosity metric provides a deeper level of information regarding an individual patch that may be beneficial.

In studies of processes that yield patterns on landscapes comprised of patches, the measure of porosity provides a metric that simultaneously characterizes edge complexity and internal perforations. Such information could help quantify habitat fragmentation combined with changes to patch compactness, and the interface complexity between adjacent land cover types. Thus, having a means of measuring the outcomes of landscape processes offers an opportunity to track changes and measure deviations due to natural or anthropogenic processes influencing landscape structures and affecting the sustainability of contained flora and fauna.

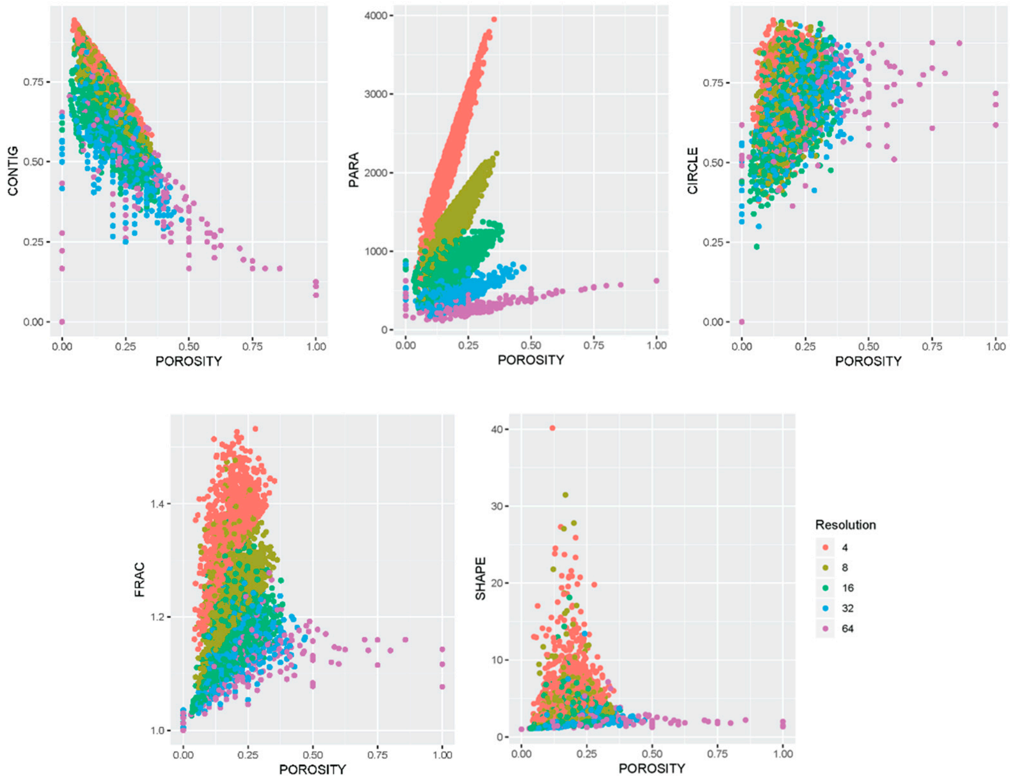

Figure 8. Scatterplots comparing the porosity metric to five leading patch-metrics from Fragstats. Data points are coloured based on their spatial resolution.

4. Conclusions

This paper presents a new metric for characterizing and comparing the complexity of 2D landscape entities that is sensitive to the internal joins of cell edges relative to a theoretical maximum given a set number of raster cells comprising that patch. Contrary to metrics married to perimeter and area measurements, the proposed porosity metric further characterizes internal perforations and edge complexity due to erosion. I demonstrated that this metric differs from popular existing metrics and that it adds to the richness of existing metrics (rather than duplicating or replacing them). The metric is robust in that it withstands rotations, mirroring, or flipping of shapes; it works for any cell size; and can potentially be used to statistically compare groups of entities based on measurements of Φ. Statistical comparisons will require further project context to establish appropriate hypotheses, and to identify valid tests. Since the method links with established methods such as mathematical morphology and join-count statistics, the tangibility and visualization of outcomes is possible, making the metric less abstract than those that are more difficult to visualize.

Two short case studies were presented to illustrate the use of this metric: (1) fabricated shapes to illustrate theoretical concepts, and (2) boreal wildfire residual vegetation patches. The porosity metric was demonstrated to capture overall shape complexity and the presence of perforations—aspects that are theoretically interesting and important. However, the assessment of residual vegetation patch porosity also showed a relatively stable level of porosity (~17.6%) when measured with up to 16 m spatial resolution imagery of these naturally occurring wildfire systems that are also left to extinguish naturally. Coarser spatial resolutions had greater variance in mean porosity value. In terms of sustainable forest management, this begins to provide a target and a range of variability that should be sought when emulating natural wildfire disturbances with forest harvesting practices. These results should be used in conjunction with measures of wildfire area, perimeter length, species distributions, and size-class distributions to best inform such practices.

Funding: This research received no external funding.

Acknowledgments: I acknowledge the anonymous reviewers who provided constructive feedback on earlier versions of this manuscript. I also thank the Forest Landscape Ecology Program of the Ontario Forest Research Institute for providing access to the base data.

Conflicts of Interest: The author declares no conflict of interest.

References

1. Kirkman, L.; Drew, M.; West, L.; Blood, E. Ecotone characterization between upland longleaf pine/wiregrass stands and seasonally-ponded isolated wetlands. *Wetlands* **1998**, *18*, 346–364. [CrossRef]
2. Long, J.; Nelson, T.; Wulder, M. Regionalization of Landscape Pattern Indices Using Multivariate Cluster Analysis. *Environ. Manag.* **2010**, *46*, 134–142. [CrossRef] [PubMed]
3. Long, J.A.; Nelson, T.A.; Wulder, M.A. Characterizing forest fragmentation: Distinguishing change in composition from configuration. *Appl. Geogr.* **2010**, *30*, 426–435. [CrossRef]
4. Botequilha Leitão, A.; Ahern, J. Applying landscape ecological concepts and metrics in sustainable landscape planning. *Landsc. Urban Plan.* **2002**, *59*, 65–93. [CrossRef]
5. da Vitoria, E.L.; Fernandes, H.C.; Teixeira, M.M.; Cecon, P.R.; Lacerda, E.D.G. Linear and spatial correlations among forage yield, bulk density and total porosity in function of soil management system. *Eng. Agríc.* **2012**, *32*, 909–919.
6. Alhusseny, A.; Turan, A. Effects of centrifugal buoyancy on developing convective laminar flow in a square channel occupied with a high porosity fibrous medium. *Int. J. Heat Mass Transf.* **2015**, *82*, 335–347. [CrossRef]
7. Eysenrode, D.S.; Bogaert, J.; Van Hecke, P.; Impens, I. Forest canopy perforation in time and space in Amazonian Ecuador. *Acta Oecol.* **2000**, *21*, 285–291. [CrossRef]
8. Manda, A.; Gross, M. Identifying and characterizing solution conduits in karst aquifers through geospatial (GIS) analysis of porosity from borehole imagery: An example from the Biscayne aquifer, South Florida (USA). *Adv. Water Resour.* **2006**, *29*, 383–396. [CrossRef]
9. Anselmetti, F.S.; Luthi, S.; Eberli, G.P. Quantitative characterization of carbonate pore systems by digital image analysis. *Am. Assoc. Pet. Geol. Bull.* **1998**, *82*, 1815–1836.
10. Hobold, G.M.; da Silva, A.K. Two-dimensional porosity optimization of saturated porous media for maximal thermal performance under forced convection. *Int. J. Heat Mass Transf.* **2017**, *108*, 1689–1701. [CrossRef]
11. Wickham, J.D.; Riitters, K.H. Sensitivity of landscape metrics to pixel size. *Int. J. Remote. Sens.* **1995**, *16*, 3585–3594. [CrossRef]
12. Chrisman, N. *Exploring Geographic Information Systems*; John Wiley & Sons, Inc.: New York, NY, USA, 1997.
13. Wade, T.G.; Wickham, J.D.; Nash, M.S.; Neale, A.C.; Riitters, K.H.; Jones, K.B. A comparison of vector and raster GIS methods for calculating landscape metrics used in environmental assessments. *Photogramm. Eng. Remote. Sens.* **2003**, *69*, 1399–1405. [CrossRef]
14. Stein, A.; Bastiaanssen, W.G.M.; De Bruin, S.; Cracknell, A.P.; Curran, P.J.; Fabbri, A.G.; Gorte, B.G.H.; Van Groenigen, J.W.; Van Der Meer, F.D.; Saldana, A. Integrating spatial statistics and remote sensing. *Int. J. Remote. Sens.* **1998**, *19*, 1793–1814. [CrossRef]
15. Lobo, A.; Moloney, K.; Chic, O.; Chiariello, N. Analysis of fine-scale spatial pattern of a grassland from remotely-sensed imagery and field collected data. *Landsc. Ecol.* **1998**, *13*, 111–131. [CrossRef]
16. Turner, M.G. Spatial simulation of landscape changes in Georgia: A comparison of 3 transition models. *Landsc. Ecol.* **1987**, *1*, 29–36. [CrossRef]
17. Keane, R.E.; Cary, G.J.; Parsons, R. Using simulation to map fire regimes: An evaluation of approaches, strategies, and limitations. *Int. J. Wildland Fire* **2003**, *12*, 309–322. [CrossRef]
18. Baker, W.L.; Cai, Y.M. The r.le-programs for multiscale analysis of landscape structure using the GRASS geographical information-system. *Landsc. Ecol.* **1992**, *7*, 291–302. [CrossRef]
19. McGarigal, K.; Marks, B.J. *FRAGSTATS: Spatial Pattern Analysis Program for Quantifying Landscape Structure*; U.S. Department of Agriculture, Forest Service, Pacific Northwest Research Station: Portland, OR, USA, 1995; p. 122.
20. Haines-Young, R.; Chopping, M. Quantifying landscape structure: A review of landscape indices and their application to forested landscapes. *Prog. Phys. Geogr.* **1996**, *20*, 418–445. [CrossRef]

21. Uuemaa, E.; Antrop, M.; Roosaare, J.; Marja, R.; Mander, Ü. Landscape metrics and indices: An overview of their use in landscape research. *Living Rev. Landsc. Res.* **2009**, *3*, 5–28. [CrossRef]
22. Birch, C.P.D.; Oom, S.P.; Beecham, J.A. Rectangular and hexagonal grids used for observation, experiment and simulation in ecology. *Ecol. Model.* **2007**, *206*, 347–359. [CrossRef]
23. Chefaoui, R.M. Landscape metrics as indicators of coastal morphology: A multi-scale approach. *Ecol. Indic.* **2014**, *45*, 139–147. [CrossRef]
24. Wulder, M.A.; White, J.C.; Gillis, M.D.; Walsworth, N.; Hansen, M.C.; Potapov, P. Multiscale satellite and spatial information and analysis framework in support of a large-area forest monitoring and inventory update. *Environ. Monit. Assess.* **2010**, *170*, 417–433. [CrossRef] [PubMed]
25. Riitters, K.H.; O'Neill, R.V.; Hunsaker, C.T.; Wickham, J.D.; Yankee, D.H.; Timmins, S.P.; Jones, K.B.; Jackson, B.L. A factor analysis of landscape pattern and structure metrics. *Landsc. Ecol.* **1995**, *10*, 23–39. [CrossRef]
26. Cushman, S.A.; McGarigal, K.; Neel, M.C. Parsimony in landscape metrics: Strength, universality, and consistency. *Ecol. Indic.* **2008**, *8*, 691–703. [CrossRef]
27. Remmel, T.K.; Csillag, F. When are two landscape pattern indices significantly different? *J. Geogr. Syst.* **2003**, *5*, 331–351. [CrossRef]
28. Remmel, T.K.; Fortin, M.-J. Categorical, class-focused map patterns: Characterization and comparison. *Landsc. Ecol.* **2013**, *28*, 1587–1599. [CrossRef]
29. Wang, X.; Blanchet, F.G.; Koper, N. Measuring habitat fragmentation: An evaluation of landscape pattern metrics. *Methods IN Ecol. Evol.* **2014**, *5*, 634–646. [CrossRef]
30. Turner, M.G. Landscape ecology: What is the state of the science? *Annu. Rev. Ecol. Evol. Syst.* **2005**, *36*, 319–344. [CrossRef]
31. Hagen, A. Fuzzy set approach to assessing similarity of categorical maps. *Int. J. Geogr. Inf. Sci.* **2003**, *17*, 235–249. [CrossRef]
32. Remmel, T.K.; Csillag, F. Mutual information spectra for comparing categorical maps. *Int. J. Remote. Sens.* **2006**, *27*, 1425–1452. [CrossRef]
33. Remmel, T.K. Investigating global and local categorical map configuration comparisons based on coincidence matrices. *Geogr. Anal.* **2009**, *41*, 113–126. [CrossRef]
34. Vogt, P.; Riitters, K.H.; Estreguil, C.; Kozak, J.; Wade, T.G. Mapping spatial patterns with morphological image processing. *Landsc. Ecol.* **2007**, *22*, 171–177. [CrossRef]
35. Soille, P.; Vogt, P. Morphological segmentation of binary patterns. *Pattern Recognit. Lett.* **2009**, *30*, 456–459. [CrossRef]
36. Fortin, M.-J.; Boots, B.; Csillag, F.; Remmel, T.K. On the role of spatial stochastic models in understanding landscape indices in ecology. *Oikos* **2003**, *102*, 203–212. [CrossRef]
37. Vogt, P.; Ferrari, J.R.; Lookingbill, T.R.; Gardner, R.H.; Riitters, K.H.; Ostapowicz, K. Mapping functional connectivity. *Ecol. Indic.* **2009**, *9*, 64–71. [CrossRef]
38. Remmel, T.K. ShrinkShape2: A FOSS toolbox for computing rotation-invariant shape spectra for characterizing and comparing polygons. *Can. Geogr.* **2015**, *59*, 532–547. [CrossRef]
39. Larsen, B.P.; Holdaway, S.J.; Fanning, P.C.; Mackrell, T.; Shiner, J.I. Shape as an outcome of formation history: Terrestrial Laser Scanning of shell mounds from far north Queensland, Australia. *Quat. Int.* **2017**, *427*, 5–12. [CrossRef]
40. Ostapowicz, K.; Vogt, P.; Riitters, K.H.; Kozak, J.; Estreguil, C. Impact of scale on morphological spatial pattern of forest. *Landsc. Ecol.* **2008**, *23*, 1107–1117. [CrossRef]
41. Moreau, G.; Fortin, D.; Couturier, S.; Duschesne, T. Multi-level functional response for wildlife conservation: The case of threatened caribou in managed boreal forests. *J. Appl. Ecol.* **2012**, *49*, 611–620. [CrossRef]
42. Rex, K.D.; Malanson, G.P. The fractal shape of riparian forest patches. *Landsc. Ecol.* **1990**, *4*, 249–258. [CrossRef]
43. Sawada, M. ROOKCASE: An Excel 97/2000 Visual Basic (VB) add-in for exploring global and local spatial autocorrelation. *Bull. Ecol. Soc. Am.* **1999**, *80*, 231–234.
44. Burgnam, M.A.; Fox, J.C. Bias in species range estimates from minimum convex polygons: Implications for conservation and options for improved planning. *Anim. Conserv.* **2003**, *6*, 19–28.
45. Salas, W.A.; Boles, S.H.; Frolking, S.; Xiao, X.; Li, C. The perimeter/area ratio as an index of misregistration bias in land cover change estimates. *Int. J. Remote. Sens.* **2003**, *24*, 1165–1170. [CrossRef]

46. Sokal, R.R.; Oden, N.L. Spatial autocorrelation in biology.1. Methodology. *Boil. J. Linn. Soc.* **1978**, *10*, 199–228. [CrossRef]
47. Cliff, A.D.; Ord, J.K. *Spatial Processes: Models and Applications*; Pion: London, UK, 1981.
48. Dale, M.R.T. *Spatial Pattern Analysis in Plant Ecology*; Cambridge University Press: Cambridge, UK, 1999; ISBN 978-0-511-61258-9.
49. Bogaert, J.; Rousseau, R.; Van Hecke, P.; Impens, I. Alternative area-perimeter ratios for measurement of 2D shape compactness of habitats. *Appl. Math. Comput.* **2000**, *111*, 71–85. [CrossRef]
50. Saberi, A.A. Recent advances in percolation theory and its applications. *Phys. Rep.* **2015**, *578*, 1–32. [CrossRef]
51. Gardner, R.H.; Milne, B.T.; Turner, M.G.; O'Neill, R.V. Neutral models for the analysis of broad-scale landscape pattern. *Landsc. Ecol.* **1987**, *1*, 19–28. [CrossRef]
52. Malarz, K.; Galam, S. Square-lattice site percolation at increasing ranges of neighbor bonds. *Phys. Rev. E* **2005**, *71*. [CrossRef] [PubMed]
53. With, K.A.; Crist, T.O. Critical thresholds in species' responses to landscape structure. *Ecology* **1995**, *76*, 2446–2459. [CrossRef]
54. Fahrig, L. Effects of habitat fragmentation on biodiversity. *Annu. Rev. Ecol. Evol. Syst.* **2003**, *34*, 487–515. [CrossRef]
55. McGarigal, K.; Cushman, S.A.; Ene, E. *FRAGSTATS: Spatial Pattern Analysis Program for Categorical and Continuous Maps*; University of Massachusetts: Amherst, MA, USA, 2012.
56. Bribiesca, E. An easy measure of compactness for 2D and 3D shapes. *Pattern Recognit.* **2008**, *41*, 543–554. [CrossRef]
57. Upton, G.J.G.; Fingleton, B. *Spatial Data Analysis by Example*; John Wiley & Sons Inc.: Toronto, ON, Canada, 1985; Volume 2.
58. Bribiesca, E. Measuring 2-D shape compactness using the contact perimeter. *Comput. Math. Appl.* **1997**, *33*, 1–9. [CrossRef]
59. Remmel, T.K.; Perera, A.H. Mapping natural phenomena: Boreal forest fires with non-discrete boundaries. *Cartographica* **2009**, *44*, 274–288. [CrossRef]
60. R Core Team. *R: A Language and Environment for Statistical Computing*; R Foundation for Statistical Computing: Vienna, Austria, 2018.
61. Perera, A.H.; Buse, L.J.; Weber, M.G. (Eds.) *Emulating Natural Forest Landscape Disturbances: Concepts and Applications*; Columbia University Press: New York, NY, USA, 2004.
62. Araya, Y.H.; Remmel, T.K.; Perera, A.H. Residual vegetation patches within natural boreal wildfires: Characterizing by pattern metrics, land cover expectations, and proximity to firebreak features. *Geomatica* **2015**, *69*, 327–338. [CrossRef]
63. Araya, Y.H.; Remmel, T.K.; Perera, A.H. Spatially explicit prediction of residual vegetation patch occurrence within boreal wildfires. *Int. J. Geoinform.* **2016**, *12*, 1–15.
64. Wu, J.G. Effects of changing scale on landscape pattern analysis: Scaling relations. *Landsc. Ecol.* **2004**, *19*, 125–138. [CrossRef]
65. Turner, M.G.; O'Neill, R.V.; Gardner, R.H.; Milne, B.T. Effects of changing spatial scale on the analysis of landscape pattern. *Landsc. Ecol.* **1989**, *3*, 153–162. [CrossRef]